

INTERNATIONAL SOCIETY FOR SOIL MECHANICS AND GEOTECHNICAL ENGINEERING



This paper was downloaded from the Online Library of the International Society for Soil Mechanics and Geotechnical Engineering (ISSMGE). The library is available here:

<https://www.issmge.org/publications/online-library>

This is an open-access database that archives thousands of papers published under the Auspices of the ISSMGE and maintained by the Innovation and Development Committee of ISSMGE.

Measurements on Model Struttéd Sheet Pile Excavations

Mesures sur modèle réduit d'une excavation étagée par des palplanches

by P. W. ROWE, D.Sc.

and

A. BRIGGS, M.Sc. Engineering Department The University of Manchester Oxford Road, Manchester 13

Summary

The results of 29 tests with model struttéd sheet-pile excavations 3'6" deep and 7'0" long, using sand, are described. 18 pressure cells of a new type were used, together with strain gauges, deflexion, and subsidence measurements.

The results demonstrate the general principle that stress is transferred from yielding to unyielding components of a composite structure. The total active load increases with the number of struts and the subsidence decreases. There is a direct correlation between subsidence and the angle of shearing resistance mobilised and it is shown that this is not a failure problem.

Introduction

Observations of the performance of struttéd excavations have been exclusively on field structures and very often the results are analysed in terms of the *failing strength* of the retained soil.

Since the purpose of the struts is to prevent subsidence of the adjacent ground, as well as to preserve stability, and since the strutting system is generally stiffer than the soil, it has been an open question as to whether failure strains are reached in the soil and to what extent failure parameters are applicable to this problem.

As a first step the lateral pressures, bending moments and strut loads have been measured on a model struttéd wall, 3'6" high and 7'0" long using loose dry sand for the retained material. These rather artificial but ideal conditions provide a basis for the study of the principles governing the behaviour of this soil-steel composite structure.

The testing apparatus and techniques follow that of earlier work, ROWE (1956) with the addition of a soil pressure gauge, BRIGGS (1960).

Sommaire

Ce rapport présente les résultats des essais faits sur modèle réduit avec des excavations limitées par des palplanches, 2,16 m de large et d'une profondeur de 1,06 m dans du sable. 18 cellules pour mesurer la pression d'un nouveau type ont été utilisées avec des extensomètres et des mesures de flexion et de tassement.

Les résultats démontrent le principe général que dans une structure composée les contraintes sont transférées des éléments flexibles aux éléments rigides. Les pressions actives totales augmentent avec le nombre des étais qui diminuent le tassement.

Il y a un rapport direct entre le tassement et l'angle de cisaillement mobilisé et l'on a pu montrer qu'il ne s'agit pas ici d'un problème de rupture.

The soil pressure gauge Figs. 1 and 2

The deflexion of the diaphragm under pressure displaces de-aired water from a chamber behind the diaphragm. The total volume change did not exceed 0.005 cc, consistent with a diaphragm deflexion of less than 1/2000 times the diameter, and it was recorded by connecting the water chamber to a glass capillary tube of 0.25 mm internal diameter. A dummy chamber of the same volume connected to a similar glass tube provided compensation for temperature.

Each gauge was first calibrated by recording the fluid pressure applied to the diaphragm against the difference in level of the water in the two capillary tubes. It was then recalibrated under vertical pressure of sand in a large sand flume so as to avoid any possibility of side effects.

While repeated water calibrations gave consistent results, the sand calibrations were found to vary, Fig. 3. The average of the volume changes per unit pressure under sand was 94 per cent of those using water and this appears to be a normal finding with soil pressure gauges TROLLOPE and LEE (1957).

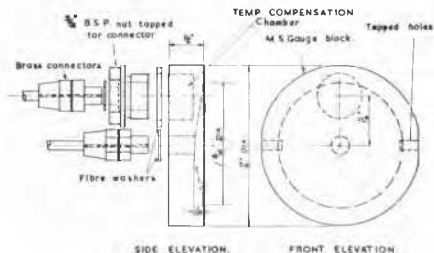


Fig. 1 Diagram of pressure cell.
Schéma de la chambre de pression.

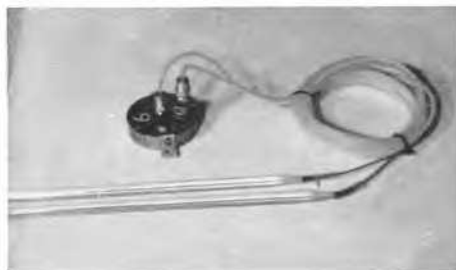


Fig. 2 Photograph of cell.
Photographie de la cellule.

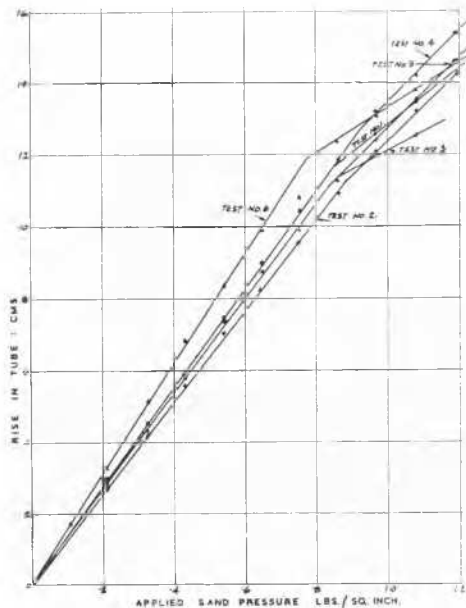


Fig. 3 Calibration curves in sand.
Courbes d'étalonnage dans le sable.

Weight and pulley arrangement to counterbalance weight of walings

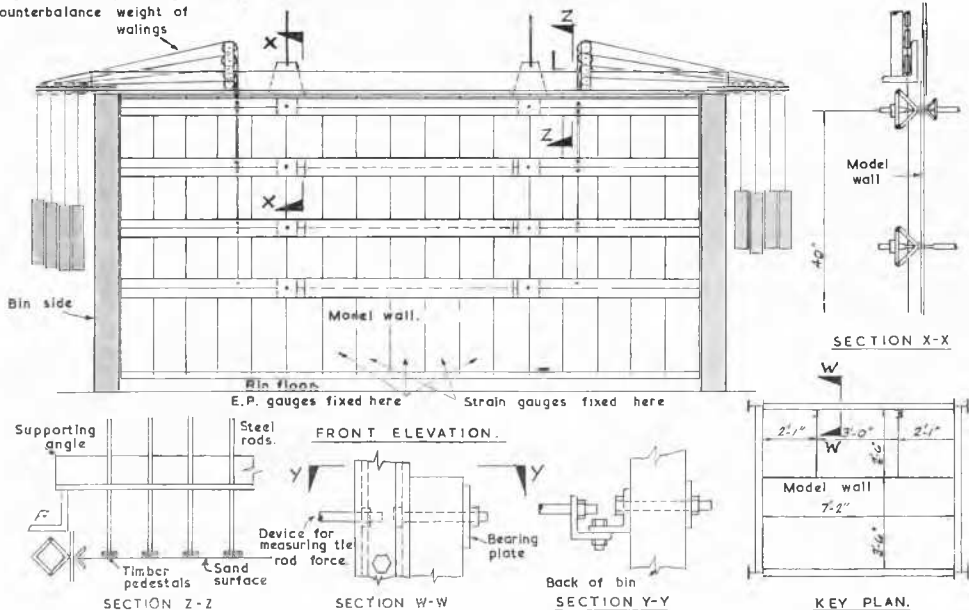


Fig. 4 Arrangement of apparatus.
Schéma de l'appareil.

The gauges were used up to a pressure of 0.7 lb./in² and were sensitive to 0.01 lb./in².

Apparatus and method of test

The sand was uniformly graded between 0.6 — 0.08 mm grain size and consisted of sub-rounded quartz particles with an average angle of friction between grains, Φ_{μ} of 25°. Other properties are given in Table 1.

Table 1

Specific Gravity	n	n. Max. per cent	n Min.	Rel. Porosity	Φ°	δ°
2.62	42.5	45	32.5	0.2	32.0	28.4

The model arrangement is illustrated in Figs. 4 and 5. The vertical spacings of the soil pressure gauges and the electrical strain gauges were so arranged that during any test, one gauge of each kind was always present at each waling level. The walings were tied to the back of the bin by two non-yielding tie rods rather than struted against the front. The weights of the walings were counterbalanced.

The wall flexibility number, —2.08, and the method of test, were arranged to simulate construction. The wall was suspended vertically in the bin which was filled evenly on both sides of the wall. Sand was then removed from the front of the wall and the walings were inserted as each tie level was uncovered. In a number of tests the struts were prestressed to an equivalent load of 2 tons per ft. run on a 40 ft. sheet pile.

A total number of 29 tests were made using one, two, three



Fig. 5 Photograph of apparatus.
Photographie de l'appareil.

and four equally spaced walings at values of excavation depth to sheet pile length, α , equal to 0.7, 0.8 and 0.9.

Experimental results

Typical bending moment distributions are shown in Figs. 6, 7 and 8. The term Z denotes depth below the top of the sheeting, height H . The bending moments have been divided by H^3 to give a number independent of scale.

Earth pressure distributions are given in Figs. 9 - 12, together with the strut loads. Some subsidence profiles are shown in Fig. 13.

Discussion of results

Previous work, Rowe (1952) on a stiff model sheet pile with unyielding anchorage proved a concentration of pressure at the anchor level and a decrease in pressure towards the centre of the wall. Fig. 9 shows that with a flexible wall this effect is more pronounced. In each case the total active load is consistent with the use of the classical earth pressure diagram using failure parameters.

In the tests with more than one waling, concentrations of pressure occur at each waling level. The pressure diagrams illustrate the general principle that when parts of a composite

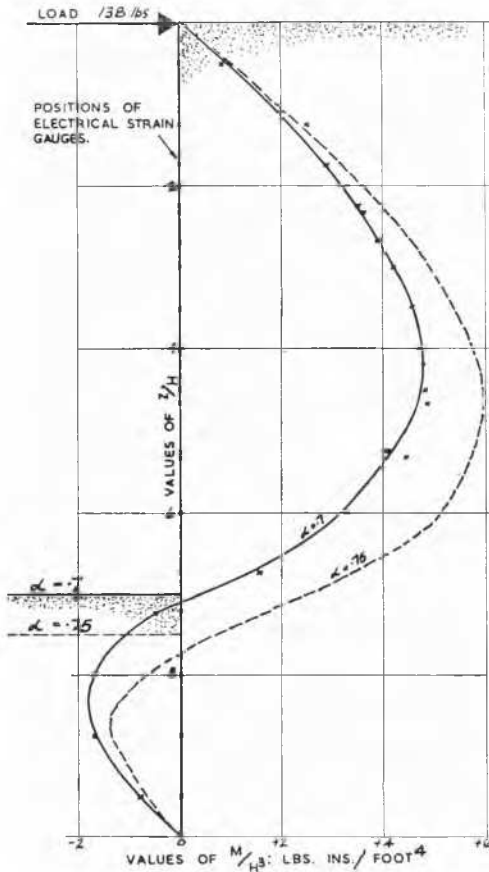


Fig. 6 Bending moment distribution 1 waling.
Répartition du moment fléchissant.

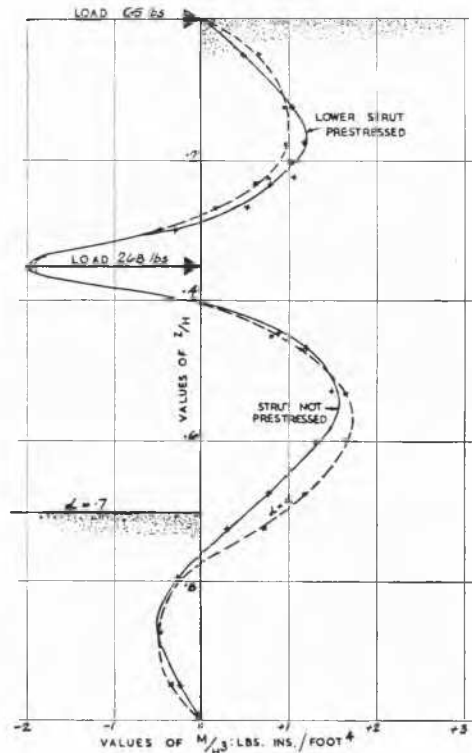


Fig. 7 Bending moment distribution 2 walings.
Répartition du moment fléchissant.

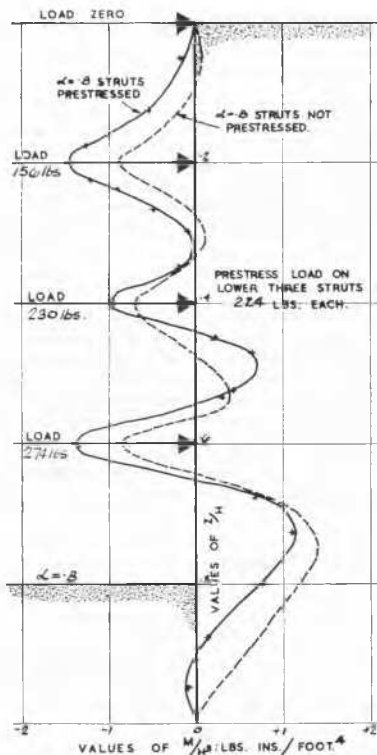


Fig. 8 Bending moment distribution 3 walings.
Répartition du moment fléchissant.

structure start to yield, the stresses are transferred to the unyielding components.

The total active and passive loads were measured from the earth pressure diagrams. In Table II the loads are balanced against the measured strut loads and the calculated maximum

Table II

Type of Test	Waling Load lbs.	Sand Passive Force lbs.	Toe Friction Force lbs.	Sum of Resisting Forces lbs.	Total Active Force lbs.	Difference per cent
Walling						
$\alpha = 0.7$ 1	138	692	83	913	828	- 10.3
$\alpha = 0.7$ 2	333	398	185	916	882	- 2.6
$\alpha = 0.8$ 2	494	264	238	996	930	- 7.1
$\alpha = 0.9$ 2	652	218	269	1139	990	- 15.0
$\alpha = 0.7$ 3	375	328	222	925	940	+ 1.6
$\alpha = 0.8$ 3	512	286	243	1041	970	- 7.3
$\alpha = 0.9$ 3	717	141	317	1175	1080	- 8.8
$\alpha = 0.7$ 4	379	324	250	953	1030	+ 7.5
$\alpha = 0.8$ 4	538	266	265	1069	1025	- 4.3
$\alpha = 0.9$ 4	670	162	316	1148	1095	- 4.8

Average - 5.1

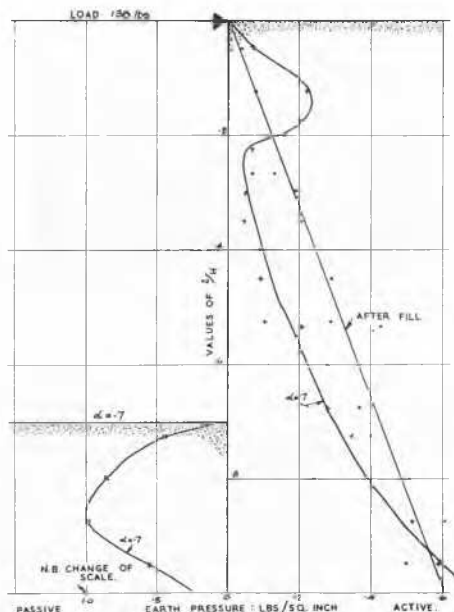


Fig. 9 Earth pressure distribution 1 waling.
Répartition de la poussée des terres.

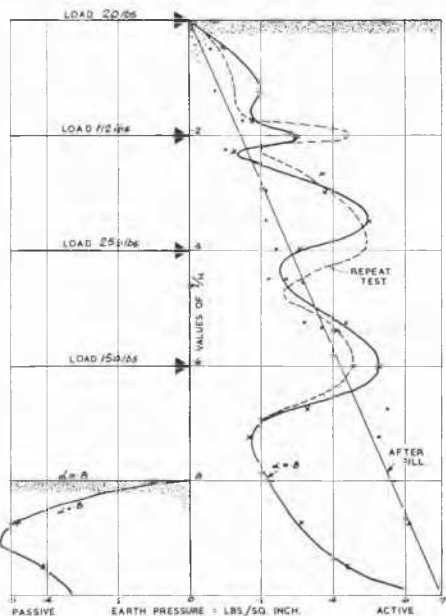


Fig. 10 Earth pressure distribution 2 walings.
Répartition de la poussée des terres.

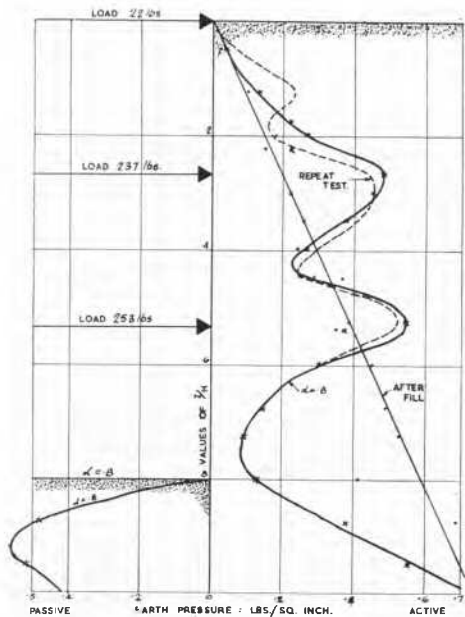


Fig. 11 Earth pressure distribution 3 waling.
Répartition de la poussée des terres.

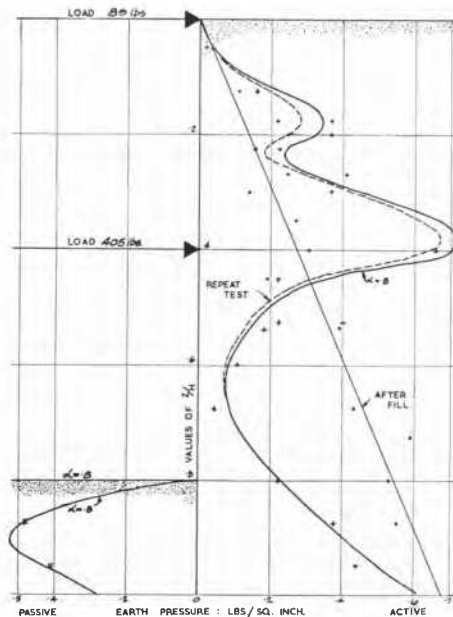


Fig. 12 Earth pressure distribution 4 waling.
Répartition de la poussée des terres.

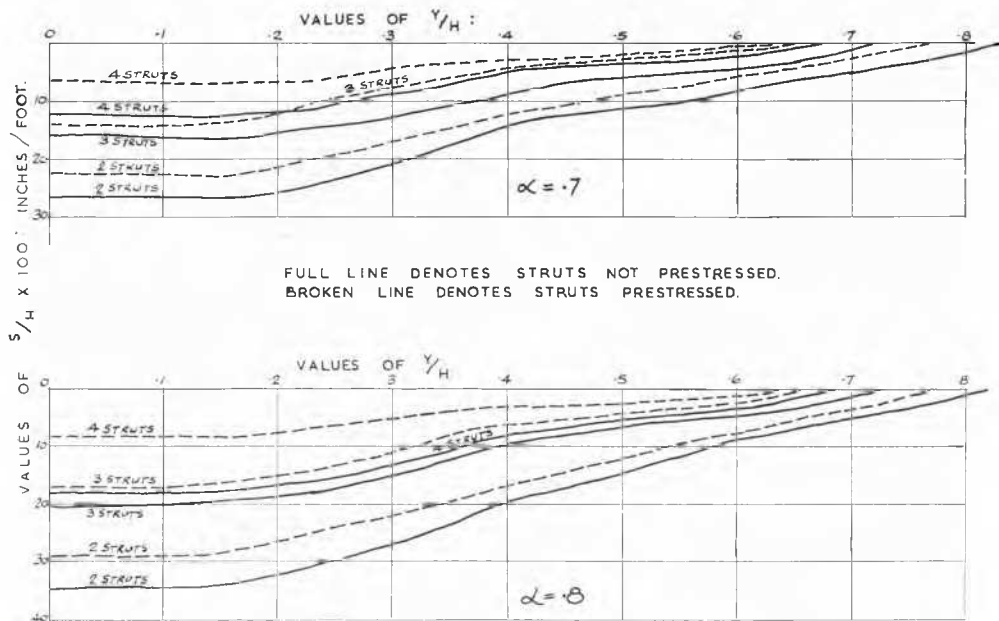


Fig. 13 Observed sand subsidence.
Tassements du sable observés.

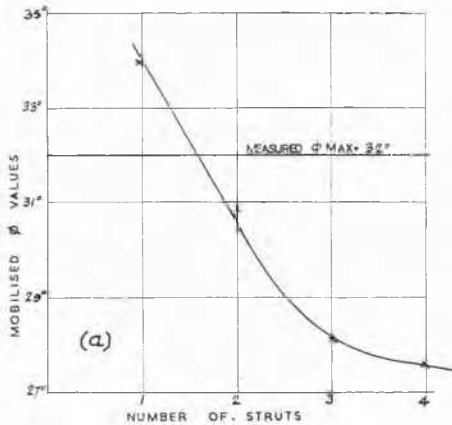


Fig. 14 Variation of number of struts with Φ mobilised.
Variation du nombre d'étais en fonction de la mobilisation de Φ .

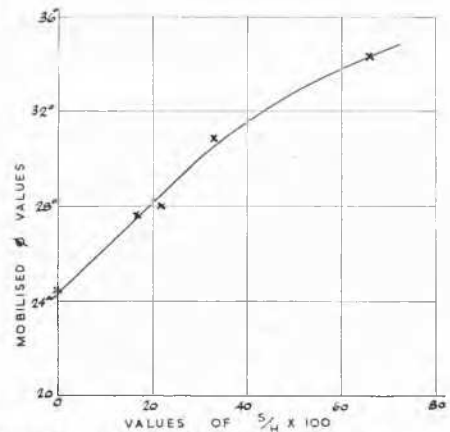


Fig. 15 Variation of subsidence with Φ mobilised.
Variation du tassement en fonction de la mobilisation de Φ .

toe shear force. The sheeting was not failing at the toe and the average error in the balance was -5 per cent. This average error would be zero if $\delta = 24 \frac{1}{2}^\circ$ were mobilised at the toe. Table III gives the mean active loads obtained with one, two three and four walings respectively and also just after the bin had been filled. The values in column 3 were obtained by dividing those in column 2 by the term $\frac{1}{2} \gamma H^2 L$, where L was the model width (7.16 feet). The mobilised Φ values, column 4 were calculated using Coulomb's equation with maximum wall friction. During the filling of the bin the confined compression of the sand also induces full wall friction.

The essential findings are illustrated in Figs. 14 and 15. An increase in the number of struts clearly decreases the

deflexion of the wall and therefore the strains imposed on the soil. Consequently the mobilised angle of shearing resistance is also decreased. There is a direct relation between the subsidence and the angle of shearing resistance mobilised, Fig. 15. Prestressing the struts induces lateral deformation and reduces the subsidence in this case to about one quarter of that without prestressing. The final active loads were only slightly increased.

Conclusion

These tests clearly illustrate the need to differentiate between deformation and failure problems. With one strut, as in a sheet pile wall, the total active load can be calculated on the basis of failure, although the passive fixity is not a failure calculation. However with several struts, the purpose of which is to prevent adjacent soil deformation, not even the active load may be computed on the basis of the failure parameters of the soil. This is a principle which may be expected to apply in varying degrees to all soils.

Table III

1 Number of Walings	2 Mean Active Load. lbs.	3 Equivalent K_a Value	4 Mobilised Φ° Values
1	828	.224	34.0
2	934	.252	30.9
3	996	.279	28.1
4	1050	.284	27.6
Bin Full No. Wall deflexion	1190	.320	24.5

References

- [1] BRIGGS, A. (1960). Struttred Sheet Pile Excavations in Cohesionless Materials. *M.Sc. Thesis University of Manchester*.
- [2] ROWE, P. W. (Jan., 1952). Anchored Sheet Pile Walls. *Proc. Instn. Civ. Engrs.* London, Part I.
- [3] — (May, 1956). Sheet Pile Walls at Failure. *Proc. Instn. Civ. Engrs.* London, Part I.
- [4] TROLLOPE and LEE (1957). The performance of a laboratory earth pressure cell. *Australian Journal of Applied Science*.